Available online at www.sciencedirect.com
SCIENCE DIRECT
Biochimica et Biophysica Acta 1758 (2006) 13 – 19
BIOCHIMICA ET BIOPHYSICA ACTA
BBA
http://www.elsevier.com/locate/bba

Functional and molecular characterization of adenosine transport at the rat inner blood–retinal barrier

Katsuhiko Nagase [a,b], Masatoshi Tomi [a], Masanori Tachikawa [a], Ken-ichi Hosoya [a,*]

[a] Faculty of Pharmaceutical Sciences, University of Toyama, 2630, Sugitani, Toyama 930-0194, Japan
[b] Department of Hospital Pharmacy, School of Medicine, Kanazawa University, 13-1, Takara-machi, Kanazawa 920-8641, Japan

Received 9 May 2005; received in revised form 6 December 2005; accepted 11 January 2006
Available online 2 February 2006

Abstract

The purpose of the present study was to characterize the adenosine transport system(s) at the inner blood–retinal barrier (inner BRB). A conditionally immortalized rat retinal capillary endothelial cell line (TR-iBRB2), used as an in vitro model of the inner BRB, expresses equilibrative nucleoside transporter 1 (ENT1), ENT2, concentrative nucleoside transporter 2 (CNT2), and CNT3 mRNAs. TR-iBRB2 cells exhibited an Na^+-independent and concentration-dependent [^{3}H]adenosine uptake with a Michaelis–Menten constant of 28.5 μM and a maximum uptake rate of 814 pmol/(min mg protein). [^{3}H]Adenosine uptake by TR-iBRB2 cells was strongly inhibited by 2 mM adenosine, inosine, uridine, and thymidine. On the other hand, this process was not inhibited by 100 nM nitrobenzylmercaptopurine riboside and dipyridamole. These uptake studies suggest that ENT2 is involved in [^{3}H]adenosine uptake by TR-iBRB2 cells. Quantitative real-time PCR revealed that the expression of ENT2 mRNA is 5.5-fold greater than that of ENT1 mRNA. An in vivo study suggested that [^{3}H]adenosine is transported from the blood to the retina and significantly inhibited by adenosine and thymidine. The results of this study show that ENT2 most likely mediates adenosine transport at the inner BRB and is expected to play an important role in regulating the adenosine concentration in the retina.

Keywords: Blood–retinal barrier; Adenosine; Nucleoside transporter

1. Introduction

Adenosine is an important intercellular signaling molecule and it plays a number of roles in retinal neurotransmission, blood flow, vascular development, and response to ischemia [1,2]. These effects are mediated through cell-surface adenosine receptors, so that the effect of adenosine in the retina is markedly influenced by the adenosine concentration in the retinal interstitial fluid. Most of the adenosine in the retinal interstitial fluid is thought to originate from the catabolism of adenosine monophosphate catalyzed by membrane-bound ecto-5′-nucleotidase (CD73) [1], which is localized in the innermost process of Müller cells [3]. Consequently, almost all of the retinal adenosine is distributed in the neighborhood of the innermost process of Müller cells in the ganglion cell layer, inner plexiform layer, and inner nuclear layer [4]. Retinal blood vessels are also distributed in ganglion cell layer, inner and outer plexiform layers, and inner nuclear layer [5] and form the inner blood–retinal barrier (inner BRB) which strictly regulates molecular transport between the blood and the retinal interstitial fluid [6]. Polska et al. [7] have reported that exogenous adenosine introduced via infusion increases the optic nerve head blood flow in healthy humans. Since adenosine in the blood needs to penetrate the inner BRB in order to activate its receptors expressed in vascular smooth muscle cells and increase blood flow, it has been suggested that adenosine transport system(s) at the inner BRB also have the ability to regulate the adenosine concentration in the retinal interstitial fluid and modulate retinal functions.

Two classes of nucleoside transporters have been described. The Na^+-independent equilibrative nucleoside transporter

Abbreviations: BRB, blood–retinal barrier; TR-iBRB2, conditionally immortalized rat retinal capillary endothelial cell line; NBMPR, nitrobenzylmercaptopurine riboside; ENT, equilibrative nucleoside transporter; CNT, concentrative nucleoside transporter; ECF, extracellular fluid; V_d, apparent retina-to-plasma concentration ratio; R_B, apparent blood-to-plasma concentration ratio; $K_{in,\ retina}$, apparent retinal uptake clearance of [^{3}H]adenosine; RUI, retinal uptake index; BBB, blood–brain barrier

* Corresponding author. Tel.: +81 76 434 7505; fax: +81 76 434 5172.
E-mail address: hosoyak@ms.toyama-mpu.ac.jp (K. Hosoya).

0005-2736/$ - see front matter © 2006 Elsevier B.V. All rights reserved.
doi:10.1016/j.bbamem.2006.01.011

(ENT) consists of ENT1 (Slc29a1) and ENT2 (Slc29a2) [8] while the Na^+-dependent concentrative nucleoside transporter (CNT) consists of CNT1 (Slc28a1), CNT2 (Slc28a2), and CNT3 (Slc28a3) [9]. They affect the concentration of adenosine available to its receptors in some organs. The inhibition of ENT1-mediated transport by the selective inhibitor, nitrobenzylmercaptopurine riboside (NBMPR), and consequent elevation of the adenosine concentration modulates glutamatergic synaptic transmission via presynaptic A_1 receptors in the superficial dorsal horn of the spinal cord in rats [10]. Moreover, the A_1 receptor-mediated chronotropic effect of adenosine is potentiated by the ENT1 inhibitor, dipyridamole, in the sinoatrial node of the guinea pig heart [11]. In the retina, it has been reported that [^{3}H]adenosine uptake and its inhibition by NBMPR take place in the retinal ganglion cell layer and inner nuclear layer of rabbits [12] and the cultured retinal neurons and photoreceptors of the chick embryo [13]. However, there is no information at all on the nucleoside transport system at the inner BRB although it would be very useful to have more information about adenosine transport mechanisms at the inner BRB in order to understand the regulation of the adenosine concentration in the neural retina.

The purpose of the present study was to elucidate the molecular mechanism of adenosine transport at the inner BRB. The characteristics and functions of adenosine transport at the inner BRB were examined using a conditionally immortalized rat retinal capillary endothelial cell line (TR-iBRB2) as an in vitro model of the inner BRB [14] and in vivo vascular injection techniques. TR-iBRB2 cells possess endothelial markers and glucose transporter 1 (GLUT1), P-glycoprotein, creatine transporter (CRT), and L-type amino acid transporter 1 (LAT1) [14–17], which are expressed at the inner BRB in vivo. Accordingly, TR-iBRB2 cells maintain certain in vivo functions and are a suitable in vitro model for the inner BRB.

2. Materials and methods

2.1. Animals

Male Wistar rats, weighing 250–300 g, were purchased from SLC (Shizuoka, Japan). The investigations using rats described in this report conformed to the provisions of the Animal Care Committee, Toyama Medical and Pharmaceutical University (currently University of Toyama) (#2003-48) and the ARVO Statement on the Use of Animals in Ophthalmic and Vision Research.

2.2. Cell culture

TR-iBRB2 cells were established from a transgenic rat harboring temperature-sensitive SV 40 large T-antigen gene [14]. TR-iBRB2 cells were seeded onto rat tail collagen type I-coated culture flasks (BD Biosciences, Bedford, MA). The cells were cultured in Dulbecco's modified Eagle's medium supplemented with 10% fetal bovine serum (Moregate, Bulimba, Australia) at 33 °C in a humidified atmosphere of 5% CO_2/air. The permissive temperature for TR-iBRB2 cell culture is 33 °C due to the presence of temperature-sensitive SV40 large T-antigen [14].

2.3. RT-PCR analysis

Total cellular RNA was prepared by using an Rneasy Kit (Qiagen, Hilden, Germany). Single-strand cDNA was made from total RNA by reverse transcription (RT) using oligo dT primer. The polymerase chain reaction (PCR) was performed with ENT1 (Slc29a1), ENT2 (Slc29a2), CNT1 (Slc28a1), CNT2 (Slc28a2), or CNT3 (Slc28a3) specific primers through 40 cycles of 94 °C for 30 sec, 60–62 °C for 30 sec, and 72 °C for 1 min. The sequences of the specific primers were as follows: the sense sequence was 5′-GCC AAC TAC ACA GCC CCC ATC A-3′ and the antisense sequence was 5′-TCA GCA GTC ACA GCA GGG AAC AA-3′ for rat ENT1 (GenBank accession number NM_031684), the sense sequence was 5′-CCT ACA GCA CCC TCT TCC TCA GT-3′ and the antisense sequence was 5′-CCC AGC CAA TCC ATG ACG TTG AA-3′ for rat ENT2 (GenBank accession number NM_031738) [18], the sense sequence was 5′-CAA CAC ACA GAG GCA AAG AGA GTC-3′ and the antisense sequence was 5′-CCA CAC CAG CAG CAA GGG CTA G-3′ for rat CNT1 (GenBank accession number NM_053863), the sense sequence was 5′-GGA AGA GTG ACT TGT GCA AGC TTG-3′ and the antisense sequence was 5′-GTG CTG GTA TAG AGG TCA CAG CA-3′ for rat CNT2 (GenBank accession number NM_031664), and the sense sequence was 5′-CTG TCT TTT GGG GAA TTG GAC TGC-3′ and the antisense sequence was 5′-CCA GTA GTG GAG ACT CTG TTT GC-3′ for rat CNT3 (GenBank accession number NM_080908). The PCR products were separated by electrophoresis on an agarose gel in the presence of ethidium bromide and visualized under ultraviolet light. The molecular identity of the resultant product was confirmed by sequence analysis using a DNA sequencer (ABI PRISM 310; Applied Biosystems, Foster City, CA).

2.4. [^{3}H]Adenosine uptake by TR-iBRB2 cells

The [2,8-^{3}H]adenosine ([^{3}H]adenosine, 35.9 Ci/mmol, Amersham Life Science, Buckinghamshire, UK) uptake by TR-iBRB2 cells was measured according to a previous report [15]. Briefly, TR-iBRB2 cells (1×10^5 cells/cm^2) were cultured at 33 °C for 48 hours on rat tail collagen type I-coated 24-well plates (BD Biosciences) and washed with 1 mL extracellular fluid (ECF) buffer consisting of 122 mM NaCl, 25 mM $NaHCO_3$, 3 mM KCl, 1.4 mM $CaCl_2$, 1.2 mM $MgSO_4$, 0.4 mM K_2HPO_4, 10 mM D-glucose and 10 mM HEPES (pH 7.4) at 37 °C. Uptake was initiated by applying 200 μL ECF buffer containing 0.1 μCi [^{3}H]adenosine (14 nM) at 37 °C in the presence or absence of inhibitors. Na^+-free ECF buffers were prepared by equimolar replacement of NaCl and $NaHCO_3$ with choline chloride and choline bicarbonate, respectively. After a predetermined period, uptake was terminated by removing the solution, and cells were immersed in ice-cold ECF buffer. The cells were then solubilized in 1 N NaOH and subsequently neutralized. An aliquot was taken for measurement of radioactivity and protein content using, respectively, a liquid scintillation counter (LS6500; Beckman-Coulter, Fullerton, CA) and a DC protein assay kit (Bio-rad, Hercules, CA) with bovine serum albumin as a standard.

For kinetic studies, the Michaelis–Menten constant (K_m) and maximum rate (J_{max}) of adenosine uptake were calculated from the following equation using the nonlinear least-square regression analysis program, MULTI [19].

$$J = J_{max} \times [S]/(K_m + [S]) \quad (1)$$

where [S] and J are, respectively, the concentration of adenosine and the carrier-mediated component of the uptake rate of adenosine at 5 min estimated by subtracting the uptake rate in the presence of 10 mM non-radiolabeled adenosine, which represents a non-saturable component of the uptake rate.

2.5. Quantitative real-time PCR

Quantitative real-time PCR was performed using an ABI PRISM 7700 sequence detector system (Applied Biosystems) with 2× SYBR Green PCR Master Mix (Applied Biosystems) according to the manufacturer's protocol. To quantify the amount of specific mRNA in the samples, a standard curve was generated for each run using the plasmid (pGEM-T Easy Vector; Promega, Madison, WI) containing the gene of interest. This enabled standardization of the initial mRNA content of cells relative to the amount of β-actin. The PCR was performed using ENT1, ENT2, or β-actin-specific primers and the cycling parameters are those given above. The sequences of the specific primers of rat β-actin (GenBank accession number NM_031144) were as follows: sense, 5′-TCA TGA AGT GTG ACG TTG ACA TCC GT-3′ and antisense, 5′-CCT AGA AGC ATT TGC GGT GCA CGA TG-3′.

2.6. Blood-to-retina [^{3}H]adenosine transport studies

The apparent retinal uptake clearance of [^{3}H]adenosine ($K_{in,\ retina}$) [μL/(min g retina)] from the circulating blood to the retina was determined by integration plot analysis as described previously [15]. Briefly, the rats were anesthetized with an intramuscular injection of ketamine-xylazine (1.22 mg xylazine and 125 mg ketamine/kg) and then [^{3}H]adenosine (12 μCi/head) was injected into the femoral vein. After collection of blood samples, rats were decapitated, and the retinas were removed. The retinas were dissolved in 2 N NaOH and subsequently neutralized. The radioactivity was measured in a liquid scintillation counter. As an index of the retinal distribution characteristics of [^{3}H]adenosine, the apparent retina-to-plasma concentration ratio (V_d) was used. This ratio [$V_d(t)$] (mL/g retina) was defined as the amount of [^{3}H] per gram retina divided by that per milliliter plasma, calculated over the time-period of the experiment (t). The apparent blood-to-plasma concentration ratio (R_B) was also measured to examine the [^{3}H]adenosine uptake into the blood cells. The $K_{in,\ retina}$ can be described by following Eq. (2):

$$V_d(t) = K_{in,\ retina} \times \mathrm{AUC}(t)/C_p(t) + V_i \quad (2)$$

where AUC(t) (dpm min/mL), $C_p(t)$ (dpm/mL), and V_i (mL/g retina) represent the area under the plasma concentration time curve of [^{3}H]adenosine from time 0 to t, the plasma [^{3}H]adenosine concentration at time t, and the rapidly equilibrated distribution volume of [^{3}H]adenosine in the retina, respectively. V_i is usually comparable with the vascular volume of the retina.

The inhibitory effect of nucleosides on the blood-to-retina transport of [^{3}H]adenosine was evaluated by the retinal uptake index (RUI) method [20,21]. Briefly, the rats were anesthetized with an intramuscular injection of ketamine-xylazine and then 200 μL of injection solution was injected into the common carotid artery. The injection solution consisted of Ringer–HEPES buffer (141 mM NaCl, 4 mM KCl, 2.8 mM $CaCl_2$, 10 mM HEPES, pH 7.4) which contained both a test compound, 10 μCi [^{3}H]adenosine or D-[1-^{3}H(N)]mannitol ([^{3}H]D-mannitol, 17 Ci/mmol, PerkinElmer Life Sciences, Boston, MA), and a reference compound, 0.1 μCi n-[1-^{14}C]butanol ([^{14}C]n-butanol, 2 mCi/mmol, American Radiolabeled Chemicals, St. Louis, MO), in the presence or absence of inhibitors. Rats were decapitated at 15 sec after injection, and the retina was removed. The retina was dissolved in 2 N NaOH and subsequently neutralized. The radioactivity was measured in a liquid scintillation counter. In this study, the RUI value was used as an index of the retinal distribution characteristics of [^{3}H]adenosine and can be described by following Eq. (3):

$$\mathrm{RUI} = \frac{[^3\mathrm{H}]/[^{14}\mathrm{C}](\text{dpm in the retina})}{[^3\mathrm{H}]/[^{14}\mathrm{C}](\text{dpm in the injection solution})} \times 100 \quad (3)$$

2.7. Data analysis

Unless otherwise indicated, all data represent means±S.E.M. An unpaired, two-tailed Student's t-test was used to determine the significance of differences between two groups. Statistical significance of differences among means of several groups was determined by one-way analysis of variance followed by the modified Fisher's least-squares difference method.

3. Results

3.1. Expression of nucleoside transporters in TR-iBRB2 cells

RT-PCR analysis was performed to examine the expression of ENT and CNT mRNAs in the rat retina and TR-iBRB2 cells. As shown in Fig. 1, the expression of ENT1, ENT2, CNT1, and CNT2 in the retina was detected at 431, 562, 479, and 298 bp, respectively. Of the four transporters, the expression of ENT1, ENT2, and CNT2 was also detected in TR-iBRB2 cells. The expression of CNT3 was not detected in the retina, however, and only a minor band of CNT3 was detected in TR-iBRB2 cells.

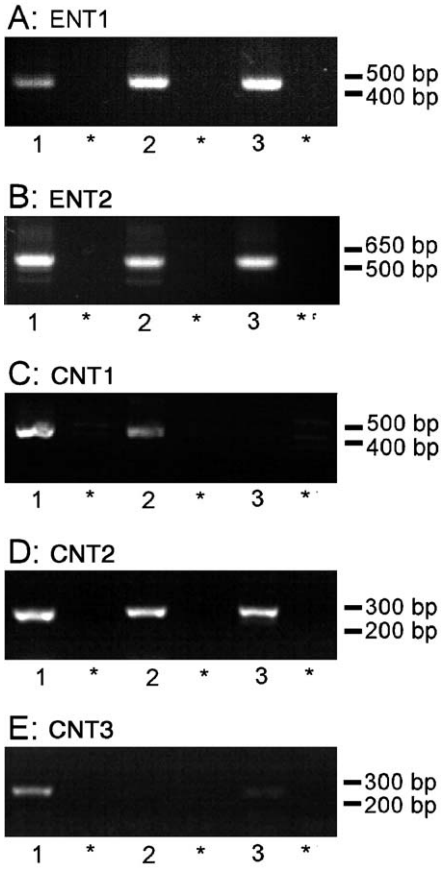

Fig. 1. RT-PCR analysis of ENT1 (A), ENT2 (B), CNT1 (C), CNT2 (D), and CNT3 (E) expression in TR-iBRB2 cells. Lane 1: positive control; lane 2: rat retina; lane 3: TR-iBRB2 cells. *: in the absence of reverse transcriptase for the respective left-hand lane. Rat brain (ENT1 and ENT2), kidney (CNT1), liver (CNT2), and small intestine (CNT3) were used as positive controls.

3.2. [^{3}H]Adenosine uptake by TR-iBRB2 cells

To analyze the kinetics and characteristics of adenosine transport at the inner BRB, [^{3}H]adenosine uptake was investigated using TR-iBRB2 cells as an in vitro model of the inner BRB. The time-courses of [^{3}H]adenosine uptake by TR-iBRB2 cells in the presence or absence of Na^+ are shown in Fig. 2. [^{3}H]Adenosine uptake increased linearly for at least 10 min. Na^+-free conditions had no effect on [^{3}H]adenosine uptake until 10 min, supporting the hypothesis that [^{3}H]adenosine uptake by TR-iBRB2 cells is predominantly mediated by ENT.

Fig. 3 shows the concentration-dependent uptake of adenosine by TR-iBRB2 cells. The Eadie–Scatchard plot (Fig. 3, inset) gave a single straight line, indicating that one saturable process was involved in adenosine uptake by TR-iBRB2 cells. Kinetic analysis of the uptake data using Eq. (1) and nonlinear least-squares regression analysis, gave a K_m of 28.5±2.2 μM and a J_{max} of 814±45 pmol/(min mg protein) (mean±S.D.).

The inhibition study was performed to characterize the [^{3}H]adenosine transport system in TR-iBRB2 cells (Table 1). Of the nucleosides studied, adenosine, inosine, uridine, and thymidine,

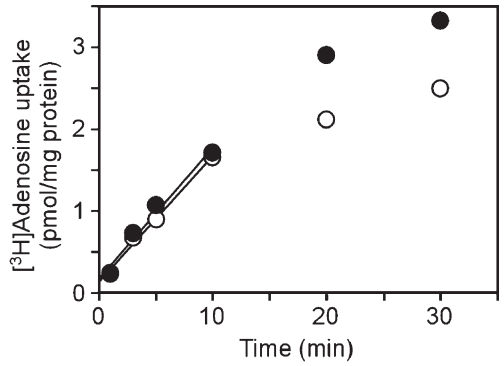

Fig. 2. Time-course of [^{3}H]adenosine uptake by TR-iBRB2 cells. The [^{3}H]adenosine (14 nM) uptake was performed at 37 °C in the presence (closed circle) or absence (open circle) of Na^+. Each point represents the mean±S.E.M. (n=4). The error bar is smaller than the size of the symbol.

at a concentration of 2 mM, inhibited [^{3}H]adenosine uptake by more than 60%, while guanosine and cytidine, at a concentration of 2 mM, partially inhibited it by up to 40%. [^{3}H]Adenosine uptake was also inhibited by nucleobases, such as 2 mM adenine and 2 mM hypoxanthine, by 41% and 28%, respectively. The Na^+-independent nucleoside transport systems can be classified according to their sensitivity to NBMPR and dipyridamole [8]. NBMPR and dipyridamole, at a concentration of 100 nM, did not inhibit [^{3}H]adenosine uptake, while NBMPR (10 and 100 μM) and dipyridamole (1 and 10 μM) produced more than 50% inhibition. These results represent NBMPR- and dipyridamole-insensitive transport of adenosine in TR-iBRB2 cells.

3.3. Expression levels of ENT1 and ENT2 in TR-iBRB2 cells

To determine the dominant ENT in TR-iBRB2 cells, quantitative real-time PCR analysis was performed to quantify the mRNA expression levels of ENT1 and ENT2 in TR-iBRB2 cells (Fig. 4). The degree of mRNA expression compensated with β-actin, for ENT1 and ENT2 was $3.27\pm0.29\times10^{-3}$ and $1.81\pm0.33\times10^{-2}$, respectively. Accordingly, the expression of ENT2 mRNA was 5.5-fold greater than that of ENT1 in TR-iBRB2 cells.

Table 1
Effect of several inhibitors on [^{3}H]adenosine uptake by TR-iBRB2 cells

	Inhibitors	Percentage of control
	Control	100±1
2 mM	Adenosine	4.75±0.13**
2 mM	Inosine	20.9±0.3**
2 mM	Uridine	35.7±1.5**
2 mM	Thymidine	24.4±0.6**
2 mM	Guanosine	60.3±1.7**
2 mM	Cytidine	70.5±3.4**
2 mM	Adenine	59.2±4.4**
2 mM	Hypoxanthine	71.8±3.8**
100 nM	Nitrobenzylmercaptopurine riboside (NBMPR)	86.3±1.9*
10 μM	NBMPR	43.9±1.8**
100 μM	NBMPR	10.5±0.6**
100 nM	Dipyridamole	92.0±1.4
1 μM	Dipyridamole	42.3±1.7**
10 μM	Dipyridamole	8.14±0.16**

[^{3}H]Adenosine uptake (14 nM) was performed in the absence (control) or presence of 2 mM inhibitors at 5 min and 37 °C. Each value represents the mean±S.E.M. (n=4–12).
* $P<0.05$ significantly different from the control.
** $P<0.001$, significantly different from the control.

3.4. Blood-to-retina transport of [^{3}H]adenosine

The in vivo blood-to-retina influx transport of adenosine from the circulating blood to the retina through the BRB was evaluated by an integration plot analysis after intravenous administration of [^{3}H]adenosine and application of the RUI method using rats. The $K_{in,\ retina}$ of [^{3}H]adenosine was found to be 25.8±0.7 μL/(min g retina) (mean±S.D.) from the slope of the integration plot (Fig. 5A). The $K_{in,\ retina}$ includes

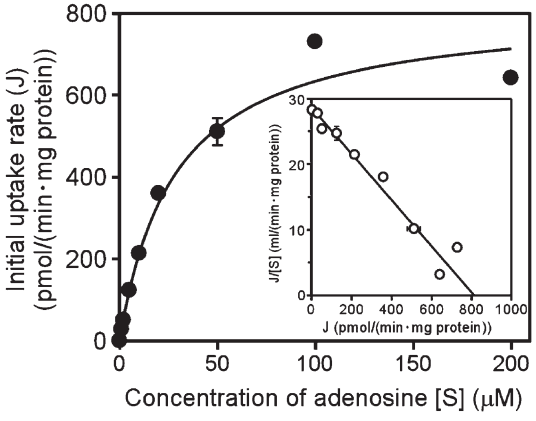

Fig. 3. Concentration-dependence of adenosine uptake by TR-iBRB2 cells. The [^{3}H]adenosine (14 nM) uptake was performed at 5 min and 37 °C. Each point represents the mean±S.E.M. (n=4). Data were subjected to Michaelis–Menten and Eadie–Scatchard analyses (inset). The K_m is 28.5±2.2 μM and J_{max} is 814±45 pmol/(min mg protein) (mean±S.D.).

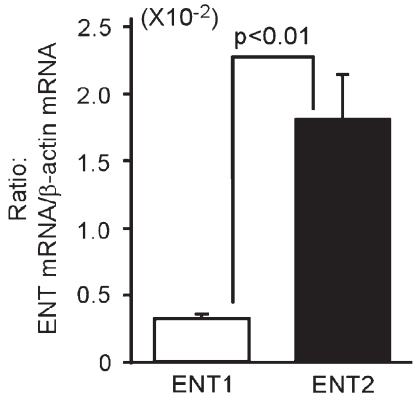

Fig. 4. The amount of ENT1 and ENT2 mRNA in TR-iBRB2 cells. The amount of ENT1 and ENT2 mRNA in TR-iBRB2 cells was determined by quantitative real-time PCR analysis. Data are the mean±S.E.M. (n=4). The quantity of ENT1 mRNA relative to β-actin mRNA (ENT1/β-actin) in TR-iBRB2 cells was $3.27\pm0.29\times10^{-3}$, and that of ENT2 mRNA (ENT2/β-actin) was $1.81\pm0.33\times10^{-2}$.

the apparent uptake clearance into the retinal blood (e.g. erythrocytes) as well as the apparent influx clearance across the BRB. In the case of adenosine, the apparent uptake clearance into the retinal blood cannot be ignored, since the R_B of [^{3}H]adenosine was increased with a slope of 0.0882 ± 0.0149 min^{-1} (mean±S.D.) (Fig. 5B). This behavior of adenosine is consistent with a previous report showing that adenosine accumulates in erythrocytes [22]. The vascular volume in the retina was found to be 0.167±0.010 mL/g retina from the V_i of [^{3}H]adenosine (Fig. 5A). By multiplying the slope of the R_B increment and the vascular volume in the retina, the apparent uptake clearance into retinal blood found to be 14.7±3.3 μL/(min g retina). Therefore, the apparent influx clearance across the BRB was found to be 11.1±4.1 μL/(min g retina). The influx transport of adenosine across the BRB was also supported by the fact that the estimated RUI value of [^{3}H]adenosine was greater than that of [^{3}H]D-mannitol (Table 2). Moreover, adenosine and thymidine at a concentration of 2 mM significantly decreased the RUI value of [^{3}H]adenosine to 70% and 75%, respectively, while 2 mM cytidine had no effect. These results confirm the carrier-mediated transport of adenosine from the blood to the retina across the BRB.

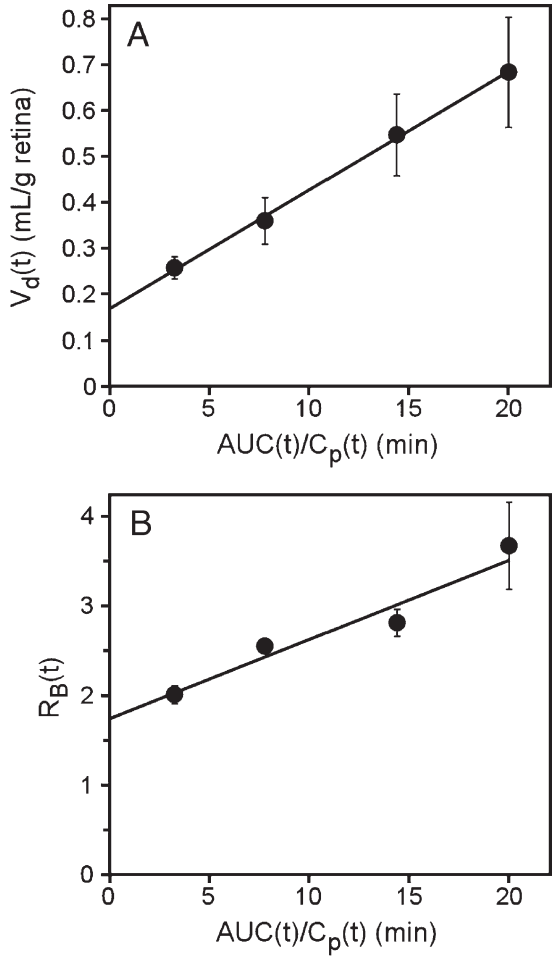

Fig. 5. Integration plot of the initial uptake of [^{3}H]adenosine by the retina (A) and blood-to-plasma concentration ratio (R_B) (B) after intravenous administration. [^{3}H]Adenosine (12 μCi/head) was injected into the femoral vein. Each point represents the mean±S.E.M. (n=3–4).

Table 2
Retinal uptake index (RUI) of [^{3}H]adenosine and [^{3}H]D-mannitol

Compounds	Inhibitors	RUI (%)	Percentage of control
[^{3}H]Adenosine		32.3±2.8	100±9
	Adenosine	22.7±3.2*	70.4±10.0*
	Thymidine	24.1±2.4*	74.7±7.3*
	Cytidine	35.0±1.7	108±5
[^{3}H]D-Mannitol		11.6±1.4	

A test compound, [^{3}H]adenosine or [^{3}H]D-mannitol (10 μCi/head), and a reference compound, [^{14}C]n-butanol (0.1 μCi/head), were injected into the common carotid artery in the presence or absence of 2 mM inhibitors. Each value represents the mean±S.E.M. (n=3–9).
* P<0.05 significantly different from the control.

4. Discussion

The present study shows that the BRB is able to transport [^{3}H]adenosine (Fig. 5). The nucleoside transporters are classified as an Na$^+$-independent ENT and an Na$^+$-dependent CNT. TR-iBRB2 cells, an in vitro model of the rat inner BRB, express both ENT and CNT mRNAs (Fig. 1), however, Na$^+$-independent uptake of [^{3}H]adenosine by TR-iBRB2 cells (Fig. 2) suggests that ENT is predominantly involved in the adenosine transport in TR-iBRB2 cells.

ENTs can be further sub-divided into two isoforms according to their sensitivity to NBMPR [8]. The NBMPR-sensitive (*es*) transporter, ENT1, is blocked by less than 100 nM NBMPR (IC_{50}=4.6 nM) [23] while the NBMPR-insensitive (*ei*) transporter, ENT2, requires more than 1 μM NBMPR to inhibit nucleoside transport [23]. Although both ENT1 and ENT2 have a variety of nucleoside substrates, ENT2 exhibits a lower affinity for guanosine and cytidine than ENT1 [24]. Moreover, only ENT2 is capable of low affinity transport of nucleobases, such as adenine and hypoxanthine [25]. In TR-iBRB2 cells, [^{3}H]adenosine uptake was not inhibited by NBMPR at 100 nM, but was inhibited at 10 and 100 μM (Table 1). [^{3}H]Adenosine uptake by TR-iBRB2 cells was inhibited by nucleosides, however, the degree of inhibition by adenosine, inosine, uridine, and thymidine was greater than that produced by guanosine and cytidine. In addition to nucleosides, [^{3}H]adenosine uptake by TR-iBRB2 cells was partly inhibited by nucleobases, such as adenine and hypoxanthine. Such forms of inhibition in TR-iBRB2 cells are consistent with ENT2 rather than ENT1. Moreover, quantitative real-time PCR analysis clearly demonstrated that ENT2 is predominantly expressed in TR-iBRB2 cells (Fig. 4). In the light of these findings, adenosine transport in TR-iBRB2 cells is most likely mediated by ENT2.

[^{3}H]Adenosine uptake by TR-iBRB2 cells was not inhibited by dipyridamole at 100 nM, but was inhibited at 1 and 10 μM (Table 1). Dipyridamole is also known to be a useful inhibitor for distinguishing human ENT1 from ENT2, since it blocks human ENT1 and ENT2 with a K_i of 5 nM and 360 nM, respectively [24]. However, in the rat, there are some contradictory reports about the ability of dipyridamole to inhibit rat ENT-mediated transport. The inhibitory effect

observed in human ENT is similar to that in rat C6 glioma cells [26] and rat brain microvascular endothelial cells [27,28] as well as the TR-iBRB2 cells in this study, while 1 μM dipyridamole had no effect on transport activity in recombinant rat ENT1 and ENT2 expressed in *Xenopus* oocytes [23]. These observations indicate that dipyridamole is an effective inhibitor of ENT2-mediated transport in the case of TR-iBRB2 cells, although its inhibitory effect seems to depend on the cell type and preparation used.

[^{3}H]Adenosine is transported from the circulating blood to the retina across the BRB with an apparent influx clearance of 11.1±4.1 μL/(min g retina) (Fig. 5). This value is far greater than that of [^{14}C]sucrose [0.26 μL/(min g retina)] and [^{3}H]D-mannitol [0.75 μL/(min g retina)] used as non-permeable paracellular markers [29]. The RUI value of [^{3}H]adenosine was also greater than that of [^{3}H]D-mannitol (Table 2). These results suggest that adenosine is transported via a carrier-mediated transport process, rather than by passive diffusion. Moreover, [^{3}H]adenosine uptake into the retina was inhibited by adenosine and thymidine, but was unaffected by cytidine (Table 2). These inhibitory characteristics are comparable with those obtained in TR-iBRB2 cells (Table 1). The BRB is composed of retinal capillary endothelial cells (inner BRB) and retinal pigment epithelial cells (outer BRB). In addition to TR-iBRB2 cells (Fig. 2), carrier-mediated adenosine transport has also been demonstrated in ARPE-19 cells, an in vitro model of the human outer BRB [30]. Accordingly, both the inner and outer BRB seem to be involved in [^{3}H]adenosine transport from the circulating blood to the retina. The net flux of adenosine transport at the BRB is still uncertain at the present time, since it is technically impossible to estimate the efflux clearance across the BRB. In the case of the blood–brain barrier (BBB), the efflux clearance of adenosine across the BBB is 3-fold greater than the influx clearance [31]. The adenosine concentration in the rat retina/choroid [32] (approximately 0.9 nmol/g ≈ 0.9 μM) is about 10-fold greater than that in the blood (90 nM) [31]. Since the K_m of adenosine uptake by TR-iBRB2 cells (28.5 μM; Fig. 3) is greater than the adenosine concentration in the retina/choroid as well as the blood, the transport velocity of adenosine at the inner BRB is expected to be relative to the adenosine concentration. Therefore, the net efflux of adenosine transport at the inner BRB may occur as at the BBB [31], since ENT2 is a bi-directional equilibrative transporter.

In conclusion, adenosine transport at the inner BRB is most likely mediated by ENT2. Under physiological conditions, adenosine serves as the principal mechanism of inhibitory neuromodulation [33]. However, the adenosine concentration is dramatically increased by more than 10-fold in the ischemic retina [32] and then adenosine exacerbates the effects of retinal ischemia/reperfusion and promotes retinal neovascularization [2,34]. Therefore, the possible physiological role for ENT2 at the inner BRB involves maintaining a constant milieu of adenosine in the retinal interstitial fluid especially under some pathological conditions like ischemia. The current findings represent an important contribution to our understanding of the physiological roles of the inner BRB in regulating the adenosine concentration in the retina.

Acknowledgements

The authors would like to thank Dr. Kazunori Katayama (University of Toyama) and Yoshiharu Deguchi (Teikyo University) for valuable discussions. This study was supported, in part, by a Grant-in-Aid for Scientific Research from the Japan Society for the Promotion of Science and a grant for Research on Sensory and Communicative Disorders by the Ministry of Health, Labor, and Welfare, Japan.

References

[1] G.A. Lutty, D.S. McLeod, Retinal vascular development and oxygen-induced retinopathy: a role for adenosine, Prog. Retin. Eye Res. 22 (2003) 95–111.
[2] G.J. Ghiardi, J.M. Gidday, S. Roth, The purine nucleoside adenosine in retinal ischemia–reperfusion injury, Vis. Res. 39 (1999) 2519–2535.
[3] G.W. Kreutzberg, S.T. Hussain, Cytochemical heterogeneity of the glial plasma membrane: 5′-nucleotidase in retinal Müller cells, J. Neurocytol. 11 (1982) 53–64.
[4] G.A. Lutty, C. Merges, D.S. McLeod, 5′ nucleotidase and adenosine during retinal vasculogenesis and oxygen-induced retinopathy, Investig. Ophthalmol. Vis. Sci. 41 (2000) 218–229.
[5] L. Sosula, P. Beaumont, K.M. Jonson, F.C. Hollows, Quantitative ultrastructure of capillaries in the rat retina, Invest. Ophthalmol. 11 (1972) 916–925.
[6] K. Hosoya, M. Tomi, Advances in the cell biology of transport via the inner blood–retinal barrier: establishment of cell lines and transport functions, Biol. Pharm. Bull. 28 (2005) 1–8.
[7] E. Polska, P. Ehrlich, A. Luksch, G. Fuchsjager-Mayrl, L. Schmetterer, Effects of adenosine on intraocular pressure, optic nerve head blood flow, and choroidal blood flow in healthy humans, Investig. Ophthalmol. Vis. Sci. 44 (2003) 3110–3114.
[8] S.A. Baldwin, P.R. Beal, S.Y. Yao, A.E. King, C.E. Cass, J.D. Young, The equilibrative nucleoside transporter family, SLC29, Pflugers Arch. 447 (2004) 735–743.
[9] J.H. Gray, R.P. Owen, K.M. Giacomini, The concentrative nucleoside transporter family, SLC28, Pflugers Arch. 447 (2004) 728–734.
[10] M.A. Ackley, R.J. Governo, C.E. Cass, J.D. Young, S.A. Baldwin, A.E. King, Control of glutamatergic neurotransmission in the rat spinal dorsal horn by the nucleoside transporter ENT1, J. Physiol. 548 (2003) 507–517.
[11] B.J. Meester, N.P. Shankley, N.J. Welsh, F.L. Meijler, J.W. Black, Pharmacological analysis of the activity of the adenosine uptake inhibitor, dipyridamole, on the sinoatrial and atrioventricular nodes of the guinea-pig, Br. J. Pharmacol. 124 (1998) 729–741.
[12] C. Blazynski, The accumulation of [^{3}H]phenylisopropyl adenosine ([3H] PIA) and [^{3}H]adenosine into rabbit retinal neurons is inhibited by nitrobenzylthioinosine (NBI), Neurosci. Lett. 121 (1991) 1–4.
[13] R. Paes de Carvalho, K.M. Braas, S.H. Snyder, R. Adler, Analysis of adenosine immunoreactivity, uptake, and release in purified cultures of developing chick embryo retinal neurons and photoreceptors, J. Neurochem. 55 (1990) 1603–1611.
[14] K. Hosoya, M. Tomi, S. Ohtsuki, H. Takanaga, M. Ueda, N. Yanai, M. Obinata, T. Terasaki, Conditionally immortalized retinal capillary endothelial cell lines (TR-iBRB) expressing differentiated endothelial cell functions derived from a transgenic rat, Exp. Eye Res. 72 (2001) 163–172.
[15] K. Hosoya, A. Minamizono, K. Katayama, T. Terasaki, M. Tomi, Vitamin C transport in oxidized form across the rat blood–retinal barrier, Investig. Ophthalmol. Vis. Sci. 45 (2004) 1232–1239.
[16] T. Nakashima, M. Tomi, K. Katayama, M. Tachikawa, M. Watanabe, T. Terasaki, K. Hosoya, Blood-to-retina transport of creatine via creatine transporter (CRT) at the rat inner blood–retinal barrier, J. Neurochem. 89 (2004) 1454–1461.
[17] M. Tomi, M. Mori, M. Tachikawa, K. Katayama, T. Terasaki, K. Hosoya, L-Type amino acid transporter 1 (LAT1)-mediated L-leucine transport at

the inner blood–retinal barrier, Investig. Ophthalmol. Vis. Sci. 46 (2005) 2522–2530.
[18] T. Kitano, H. Iizasa, T. Terasaki, T. Asashima, N. Matsunaga, N. Utoguchi, Y. Watanabe, M. Obinata, M. Ueda, E. Nakashima, Polarized glucose transporters and mRNA expression properties in newly developed rat syncytiotrophoblast cell lines, TR-TBTs, J. Cell. Physiol. 193 (2002) 208–218.
[19] K. Yamaoka, Y. Tanigawara, T. Nakagawa, T. Uno, A pharmacokinetic analysis program (multi) for microcomputer, J. Pharmacobio-dyn. 4 (1981) 879–885.
[20] Y.S. Kang, T. Terasaki, A. Tsuji, Acidic drug transport in vivo through the blood–brain barrier. A role of the transport carrier for monocarboxylic acids, J. Pharmacobio-dyn. 13 (1990) 158–163.
[21] A. Alm, P. Törnquist, The uptake index method applied to studies on the blood–retinal barrier. I. A methodological study, Acta Physiol. Scand. 113 (1981) 73–79.
[22] E. Snoeck, K. Ver Donck, P. Jacqmin, H. Van Belle, A.G. Dupont, A. Van Peer, M. Danhof, Physiological red blood cell kinetic model to explain the apparent discrepancy between adenosine breakdown inhibition and nucleoside transporter occupancy of draflazine, J. Pharmacol. Exp. Ther. 286 (1998) 142–149.
[23] S.Y. Yao, A.M. Ng, W.R. Muzyka, M. Griffiths, C.E. Cass, S.A. Baldwin, J.D. Young, Molecular cloning and functional characterization of nitrobenzylthioinosine (NBMPR)-sensitive (es) and NBMPR-insensitive (ei) equilibrative nucleoside transporter proteins (rENT1 and rENT2) from rat tissues, J. Biol. Chem. 272 (1997) 28423–28430.
[24] J.L. Ward, A. Sherali, Z.P. Mo, C.M. Tse, Kinetic and pharmacological properties of cloned human equilibrative nucleoside transporters, ENT1 and ENT2, stably expressed in nucleoside transporter-deficient PK15 cells. ENT2 exhibits a low affinity for guanosine and cytidine but a high affinity for inosine, J. Biol. Chem. 275 (2000) 8375–8381.
[25] S.Y. Yao, A.M. Ng, M.F. Vickers, M. Sundaram, C.E. Cass, S.A. Baldwin, J.D. Young, Functional and molecular characterization of nucleobase transport by recombinant human and rat equilibrative nucleoside transporters 1 and 2. Chimeric constructs reveal a role for the ENT2 helix 5–6 region in nucleobase translocation, J. Biol. Chem. 277 (2002) 24938–24948.
[26] C.J. Sinclair, C.G. LaRiviere, J.D. Young, C.E. Cass, S.A. Baldwin, F. E. Parkinson, Purine uptake and release in rat C6 glioma cells: nucleoside transport and purine metabolism under ATP-depleting conditions, J. Neurochem. 75 (2000) 1528–1538.
[27] M. Chishty, D.J. Begley, N.J. Abbott, A. Reichel, Functional characterisation of nucleoside transport in rat brain endothelial cells, NeuroReport 14 (2003) 1087–1090.
[28] F.E. Parkinson, J. Friesen, L. Krizanac-Bengez, D. Janigro, Use of a three-dimensional in vitro model of the rat blood–brain barrier to assay nucleoside efflux from brain, Brain Res. 980 (2003) 233–241.
[29] S.L. Lightman, A.G. Palestine, S.I. Rapoport, E. Rechthand, Quantitative assessment of the permeability of the rat blood–retinal barrier to small water-soluble non-electrolytes, J. Physiol. 389 (1987) 483–490.
[30] S. Majumdar, S. Macha, D. Pal, A.K. Mitra, Mechanism of ganciclovir uptake by rabbit retina and human retinal pigmented epithelium cell line ARPE-19, Curr. Eye Res. 29 (2004) 127–136.
[31] A.J. Isakovic, N.J. Abbott, Z.B. Redzic, Brain to blood efflux transport of adenosine: blood–brain barrier studies in the rat, J. Neurochem. 90 (2004) 272–286.
[32] S. Roth, P.S. Rosenbaum, J. Osinski, S.S. Park, A.Y. Toledano, B. Li, A.A. Moshfeghi, Ischemia induces significant changes in purine nucleoside concentration in the retina-choroid in rats, Exp. Eye Res. 65 (1997) 771–779.
[33] E.A. Newman, Glial cell inhibition of neurons by release of ATP, J. Neurosci. 23 (2003) 1659–1666.
[34] R.P. Mino, P.E. Spoerri, S. Caballero, D. Player, L. Belardinelli, I. Biaggioni, M.B. Grant, Adenosine receptor antagonists and retinal neovascularization in vivo, Investig. Ophthalmol. Vis. Sci. 42 (2001) 3320–3324.